On the Validation of Direct Simulation Monte Carlo Method for Low Reynolds Number Micro-Nozzle Resisto-Jets

IEPC-2017-306

Presented at the 35th International Electric Propulsion Conference
Georgia Institute of Technology – Atlanta, Georgia – USA
October 8–12, 2017

Timothy D. Holman and Michael F. Osborn
Naval Research Laboratory, Washington D.C.

In recent years there has been a growth in demand for CubeSats and as a result there has been a need to increase the efficiency in micro-propulsion resisto-jet systems. In a previous paper, a DSMC method was investigated as a numerical method for low Reynolds number micro-nozzles used for micro-propulsion resisto-jet systems. This procedure is advantageous as it accounts for viscosity and rarefied effects inside the low Reynolds number micro-nozzle. This paper discusses validation of the DSMC code with experimental results for four nozzle geometries across a range of Reynolds numbers using nitrogen propellant at different temperatures.

I. Introduction

There is a growing interest in CubeSats and CubeSat constellations due to increased access to low Earth orbit (LEO) as secondary ride share payloads. The CubeSat architecture allows organizations, such as Universities, access to space that would otherwise be prohibitively expensive. However, CubeSats are currently limited by their propulsion capabilities and tend to either de-orbit in a few months, or remain as orbital debris for lifetimes much past their intended use. If an efficient thruster can be added to the CubeSat system, the lifetime can be greatly expanded and debris requirements can be met. Considering the power and weight limitations of a CubeSat a low power micro-propulsion system is required for continued expansion of CubeSat utilization. The resisto-jet is of particular interest as it can meet the efficiency and reliability requirements of spacecraft. A resisto-jet is also easy to utilize and implement in a cost constrained system, such as CubeSats.

To meet the CubeSat requirements of low thrust over a long duration low mass, a resisto-jet must be able to operate at low chamber pressures and be small in size. Due to these requirements, the resisto-jet micro-nozzle must be able to operate efficiently within a low Reynolds number regime. In low Reynolds number flow, viscous effects dominate the flow within the nozzle. This differs greatly from the conventional high Reynolds number rocket nozzles because the boundary layer dominates the flow in the nozzle.

Historically, a conical nozzle geometry was used in early rocket engines due to their simplicity and ease of manufacturing. Bell or contour nozzles were developed in the 1950s as a more ideal geometry for flow expansion at the cost of a longer bell and a more involved fabrication process. The truncated perfect nozzle method was developed as a compromise between the performance of a full contour nozzle and the shorter bell length of a conical nozzle.[1,2] A contoured nozzle shape could be designed by the method of characteristics, as shown by Rao.[3] However, Rao's method is based on an assumption of inviscid flow so once the inviscid nozzle design is complete, a boundary-layer correction is added to compensate for viscous effects. This approach is sufficient for high Reynolds number flows where viscous effects do not dominate, but can be inaccurate to design a nozzle for low Reynolds number flow. The solution is to numerically simulate the viscous flow in a nozzle. This work is part of a larger program, see Osborn et al.[4] for a program overview, which includes an experimental program, see Williams et al.[5,6] for details, with an optical measurement of the plume, see Tuesta et al.[7] for more details.

Hussaini et al.[8] conducted a CFD design optimization in a low Reynolds number flow on both conical and contoured micro-nozzles. The Hussaini work is a nozzle geometry optimization using a parabolized Navier-Stokes (PNS) computational fluid dynamics (CFD) solver. It has been shown that CFD does not accurately capture rarefied effects, especially in the exit lip region of the nozzle.[9] The difference between DSMC and CFD increases as the chamber pressure is decreased. One of the nozzles of interest for this work is shown in Fig. 1; it is approximately 4 times smaller than the nozzle Hussaini et al. utilized. Holman et al.[10] continued work on optimization of micro-nozzles utilizing a DSMC code. This paper presents work on validating the DSMC numerical method for low Reynolds number micro-nozzles.

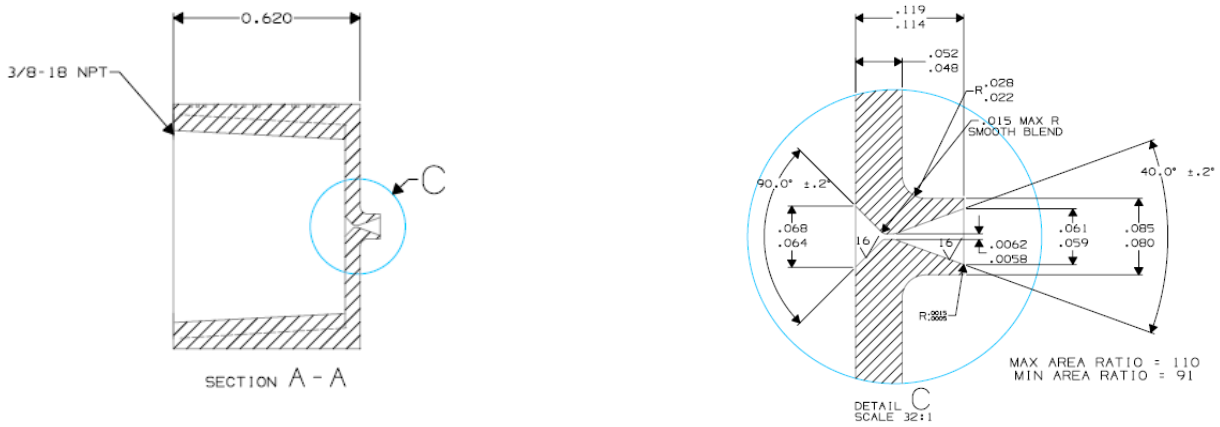

(a) Nozzle Cross Section

(b) Detail Section C

Figure 1: Diagram of Nozzle 40-100-0006 Geometry

II. Numerical Methods

Due to the nature of the micro-nozzle, several flow regimes are present from continuum flow in the chamber to rarefied flow at the nozzle exit. Figure 2 shows the variation of the Knudsen number in a resisto-jet thruster micro-nozzle. It can be seen that the Knudsen number varies from continuum to rarefied in the expansion region of the nozzle. This provides a numerical challenge, as CFD has difficulty accurately simulating high Knudsen number flows, while direct simulation monte carlo (DSMC) methods can accurately simulate high Knudsen number flows but can be numerically inefficient and therefore not ideal for this study. This study necessitated the need for a DSMC code that is capable of efficiently and accurately simulating continuum and rarefied flow.

A. DSMC Method

This study utilizes the hypersonic aerothermodynamics particle (HAP) code[11] created at the Air Force Research Laboratory for quick evaluation of DSMC algorithms and models. The HAP code includes several unique features that make the code particularly suitable for automated geometry optimization that is required for this work. The HAP code can automatically generate surface meshes around any analytically defined two- or three-dimensional solid body. For this study, the nozzle body was defined using a third order polynomial, as given in Eq. 1 below.

$$R = az^3 + bz^2 + cz + d \tag{1}$$

$$a = \frac{2}{L^3}[r_t - r_e] + \frac{1}{L^2}[r'_t + r'_e] \tag{2}$$

$$b = \frac{3}{L^2}[r_e - r_t] + \frac{1}{L}[r'_e + r'_t] \tag{3}$$

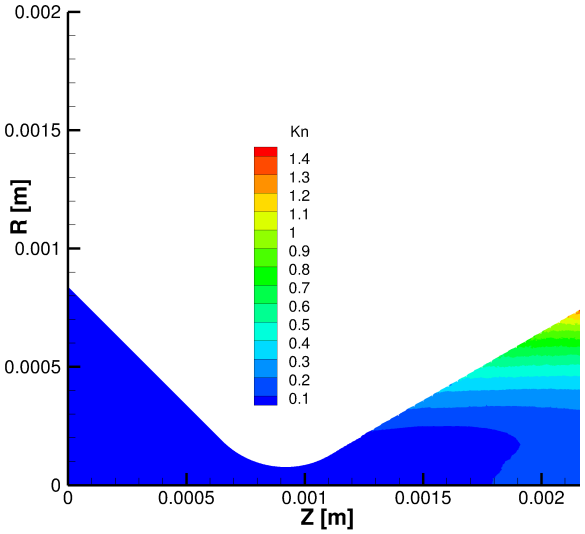

Figure 2: Knudsen Number Variation in a Resito-Jet Thruster Micro-Nozzle

$$c = r'_t \tag{4}$$

$$d = r_t \tag{5}$$

where R is the radius of the nozzle at the z axial location, r_t and r'_t is the radius and slope, respectively, at the start of the expansion region of the nozzle, r_e and r'_e is the radius and slope, respectively, at the exit of the nozzle, and L is the length of the contoured section. The above equations allows for a contoured nozzle, but the conical nozzle can be achieved by setting a=b=0.

The HAP code utilizes a Cartesian cut cell approach that has a two-level adaptive grid for sampling and a separate uniform grid for collision operations, with an option for non-uniform division of each collision cell into transient adaptive subcells. There is also an option to have transient adaptive subcells with subcell clustering in portions of a cell where the mean free path is smaller than the cell averaged value. HAP also has the ability for automated local time step adaptation. Multiple collision schemes are available, including Bird's no time counter (NTC) method which is utilized for this study. HAP also includes multiple techniques for nearest or near neighbor collision partner selection, including the use of local gradient aligned directions. It also includes a modification to collision probabilities to correct for density variation within a collision cell, allowing the cell to be much larger than the local mean free path. Selecting nearest neighbor in a gradient aligned direction while prohibiting repeated collisions can allow for a reduction in particles required with no significant effect on accuracy. All these techniques allow the HAP code to simulate a complex flow involving continuum and rarefied flow regimes with relatively low computational expense. This makes the code ideal for use in a geometry optimization of low Reynolds number micro-nozzles.

III. Results

The U.S. Naval Research Laboratory (NRL) is conducting its own experimental program in parallel with this numerical study.[4,5,6,12] The experimental program has started with four nozzles. A diagram of the cross section of the four nozzles is given in Fig. 3. The pertinent details of the geometry of the four nozzles is given in Table 1. The inlet angle for all four nozzles is 90 degrees. Each nozzle has been measured at NRL and Table 1 gives the nominal design parameters of the four nozzles and the 'as built' measured values.

The nozzles are tested with nitrogen gas at three temperatures; 295K, 423K and 523K. In addition, each nozzle is tested at 8 different flow rates which allows studying the nozzle over a range of Reynolds numbers. The results from the HAP code are compared to the experimental results for each nozzle in the following sections. Unfortunately only two nozzles, nozzle 60-100-0006 and nozzle 40-200-0006, have all the test cases

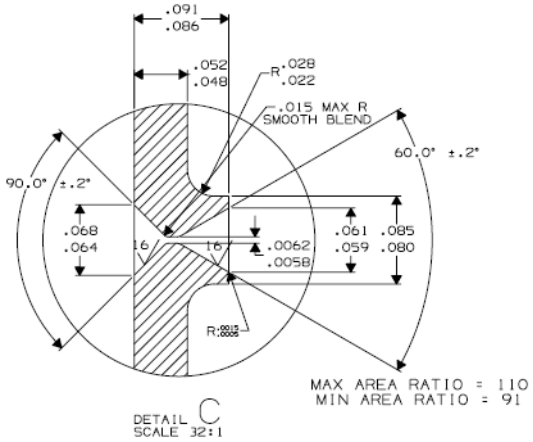

(a) 60-100-0006 Nozzle Cross Section

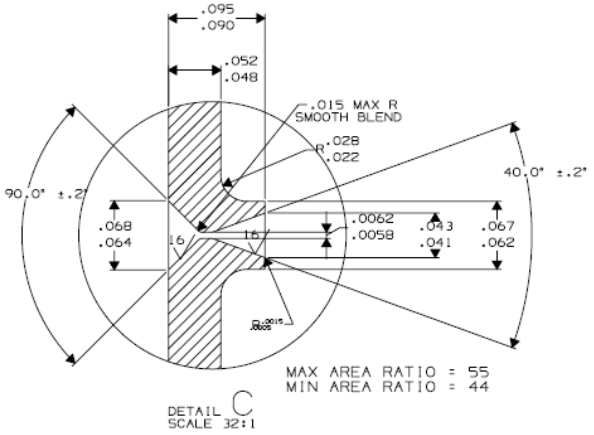

(b) 40-050-0006 Nozzle Cross Section

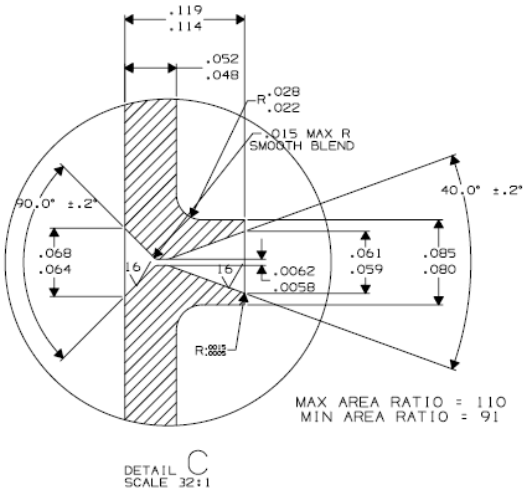

(c) 40-100-0006 Nozzle Cross Section

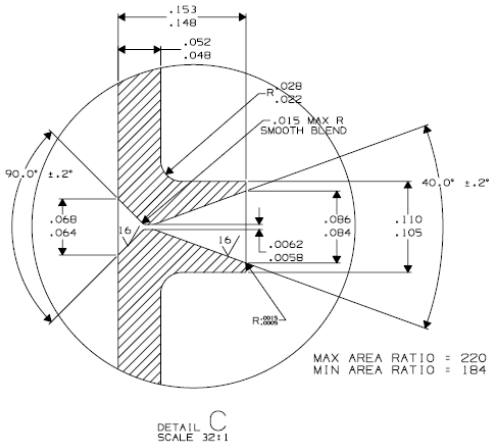

(d) 40-200-0006 Nozzle Cross Section

Figure 3: Diagram of the Four Nozzles used in this Study

Table 1: Nozzle Geometry Utilized for Verification

	Nominal Design			As Built		
Nozzle ID	Exit Angle	Area Ratio	Throat Dia.[in]	Exit Angle	Area Ratio	Throat Dia.[in]
60-100-0006	60	100	0.006	59.58	95.89	0.00626
40-050-0006	40	50	0.006	39.53	48.08	0.00598
40-100-0006	40	100	0.006	38.86	96.56	0.00591
40-200-0006	40	200	0.006	39.15	193.4	0.00591

fully simulated. The remaining two nozzles, nozzle 40-050-0006 and nozzle 40-100-0006, were not completed in time for this paper, and will be published at a later date. All results are presented as a function of throat Reynolds number and chamber temperature.

A. Nozzle 60-100-0006

The first nozzle that is discussed in this paper is the 60-100-0006 nozzle. The nozzle is a 60° conical nozzle with a nominal throat diameter of 0.006 inches (0.1524 mm) and an area ratio of 100. Figure 4 gives the experimental and numerical data for thrust and specific impulse for the three chamber temperatures: 295K, 423K, and 523K, and eight different throat Reynolds numbers.

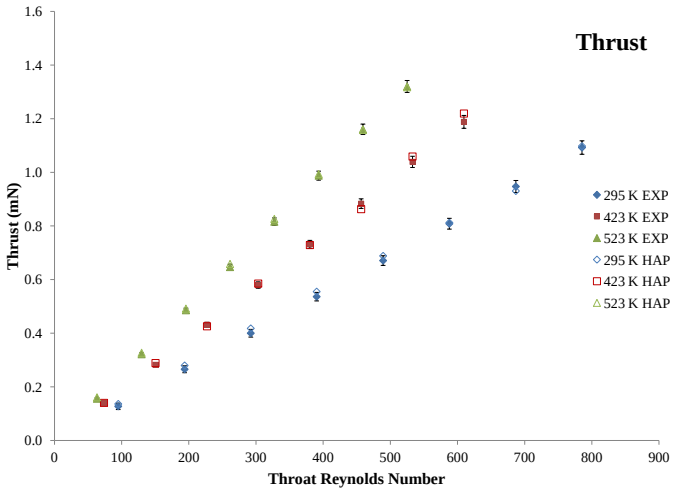

(a) Thrust

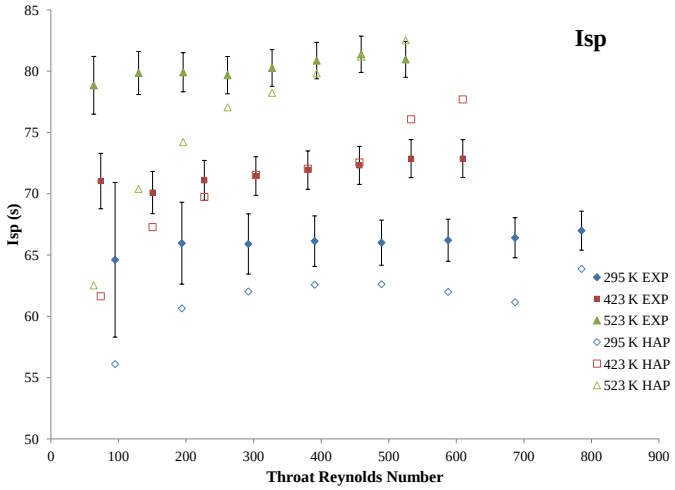

(b) Specific Impulse

Figure 4: Experimental and Numerical Thrust and Specific Impulse Comparison for the 60-100-0006 Nozzle

From Fig. 4(a) it can be seen that the experimental and numerical thrust compares well. However, from Fig. 4(b) it can be observed that the specific impulse does not compare quite as well. At lower Reynolds numbers HAP under predicts the specific impulse. As the Reynolds number rises to greater then 300, HAP predictions compare well against the experimental results for the hot cases (423K and 523K). For the cold gas case (293K), HAP under predicts the experimental result for all Reynolds numbers. At the lower Reynolds numbers, the experimental error is also the largest, but the numerical results are well outside the experimental error. It is believed the reason for this variability in specific impulse is due to the fact that specific impulse requires the thrust and mass flux be calculated, and any error in these calculations becomes

magnified in the calculation for specific impulse.

It is observed that the comparison between numerical and experimental thrust improves with increasing temperature. A higher chamber temperature means a higher temperature in the expansion portion of the nozzle, as can be observed in Fig. 5. For the cold gas cases, 295K, it was difficult to maintain more then five particles per cell while the hot gas cases, 423K and 523K, it was relatively easy to maintain more particles per cell. In general it is advised to have 10 or more particles per cell to achieve accurate results.

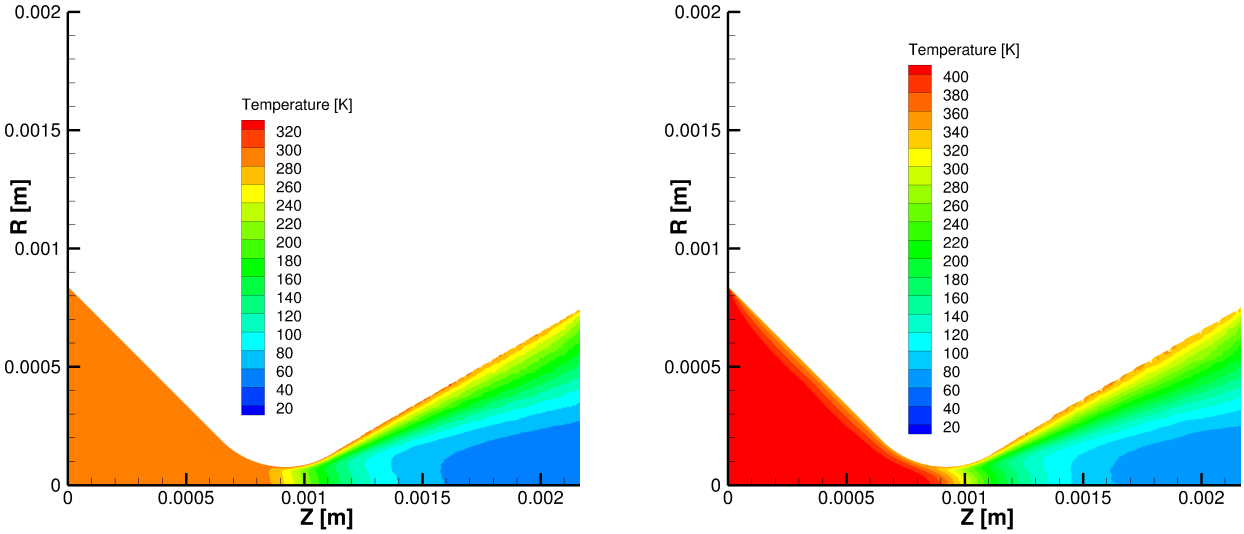

(a) 295K

(b) 423K

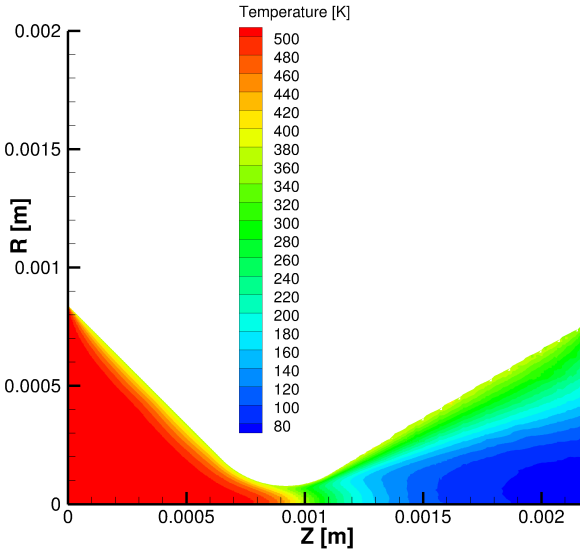

(c) 523K

Figure 5: Temperature Contours for Run 4 across the Three Temperature Cases for the 60-100-0006 Nozzle

It can also be observed from Fig. 4(a) that as the throat Reynolds number increases, the comparison between numerical and experimental thrust improves. From Fig 6, it can be seen that the number density increases with increasing Reynolds number. At low number density, it can be difficult to maintain enough particles per cell. It is believed that HAP over predicted the lower Reynolds number runs in the 293K case due to difficulty maintaining a sufficient number of particles per cell.

At higher Reynolds number, it was observed that the simulations took more iterations to reach steady state than at lower Reynolds number. The large discrepancy between HAP predicted thrust and experimental values for the last three runs for the hot gas test (423K) has no obvious explanation and remains under

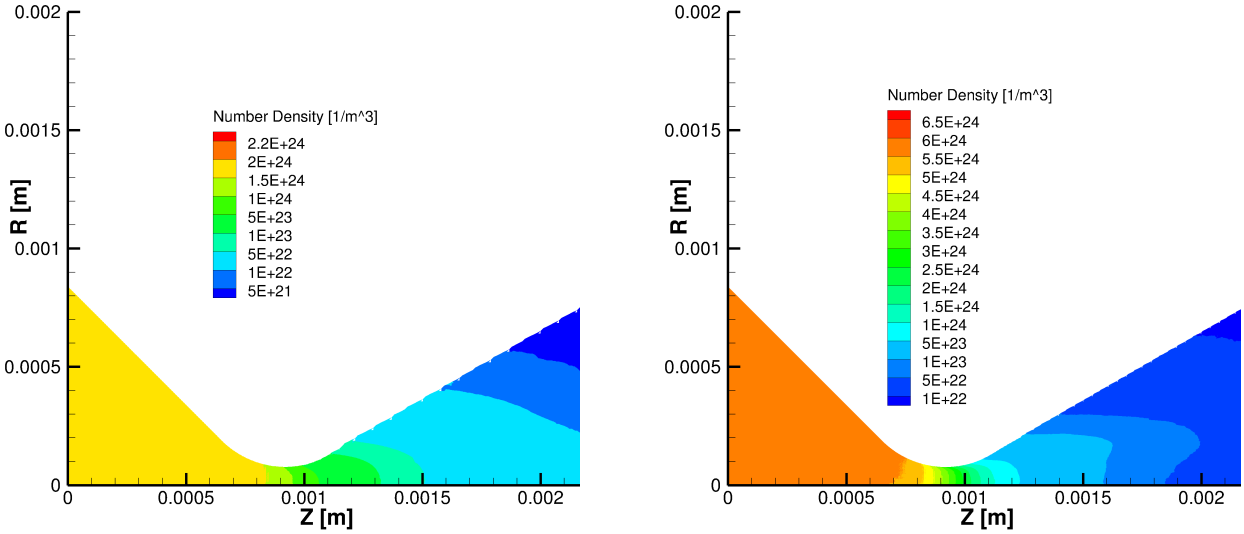

(a) Run 1

(b) Run 4

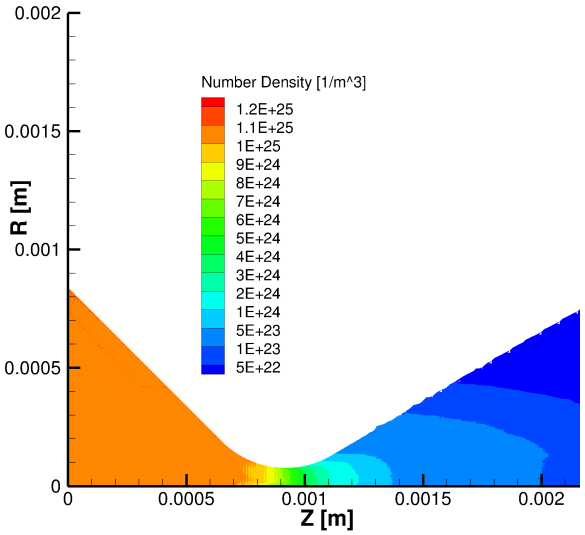

(c) Run 8

Figure 6: Number Density Contours for Cold Gas Test Case across Three Throat Reynolds Numbers for the 60-100-0006 Nozzle

investigation.

The data in table 2 gives the experimental and numerical thrust, experimental error and the difference between the numerical and experimental thrust for the three chamber temperatures and eight throat Reynolds numbers. Overall, in 15 out of 24 cases HAP predicted thrust within the margin of experimental error. The largest discrepancy is run 8 in the 423K test which over predicts the experimental result by 31 μN, but is only a little over 6 μN outside the experimental error.

Table 2: Comparison between HAP Results and Experimental Data for the 60-100-0006 Nozzle

	Cold Gas Test (295K)				
Run	Re^*	Thrust Exp [mN]	Thrust HAP[mN]	Difference [mN]	Exp Error [mN]
1	94.4	0.1275	0.1363	0.0088	0.0120
2	193.78	0.2656	0.2797	0.0141	0.0129
3	292.23	0.4002	0.4180	0.0178	0.0143
4	390.36	0.5363	0.5551	0.0188	0.0159
5	489.25	0.6709	0.6883	0.0174	0.0179
6	587.88	0.8084	0.8122	0.0038	0.0201
7	686.89	0.9471	0.9304	0.0167	0.0224
8	785.33	1.0923	1.0977	0.0055	0.0249
	Hot Gas Test (423K)				
Run	Re^*	Thrust Exp [mN]	Thrust HAP [mN]	Difference [mN]	Exp Error [mN]
1	74.74	0.1406	0.1403	0.0003	0.0028
2	150.44	0.2821	0.2888	0.0067	0.0057
3	227.06	0.4318	0.4259	0.0060	0.0087
4	303.31	0.5796	0.5852	0.0055	0.0117
5	380.23	0.7315	0.7287	0.0028	0.0147
6	456.57	0.8831	0.8626	0.0205	0.0178
7	533.06	1.0389	1.0589	0.0199	0.0209
8	609.57	1.1881	1.2192	0.0310	0.0239
	Hot Gas Test (523K)				
Run	Re^*	Thrust Exp [mN]	Thrust HAP [mN]	Difference [mN]	Exp Error [mN]
1	63.35	0.1559	0.1611	0.0052	0.0026
2	129.72	0.3216	0.3272	0.0056	0.0054
3	195.70	0.4856	0.4918	0.0062	0.0082
4	261.36	0.6467	0.6585	0.0118	0.0109
5	327.31	0.8160	0.8264	0.0104	0.0138
6	393.34	0.9877	0.9936	0.0059	0.0166
7	459.20	1.1605	1.1577	0.0028	0.0196
8	525.03	1.3201	1.3170	0.0031	0.0223

B. Nozzle 40-200-0006

The last nozzle that is discussed in this paper is the 40-200-0006 nozzle. The nozzle is a 40° conical nozzle with a nominal throat diameter of 0.006 inches (0.1524 mm) and an area ratio of 200. Figure 7 gives the experimental and numerical data for thrust and specific impulse for the three chamber temperatures and eight different throat Reynolds numbers.

From Fig. 7(a) it can be seen that the experimental and numerical thrust compares well. Most of the hot gas cases (423K and 523K) are within the experimental error. However, for the cold gas case, the numerical thrust compares well with the experimental values but only two of the eight runs are within the experimental

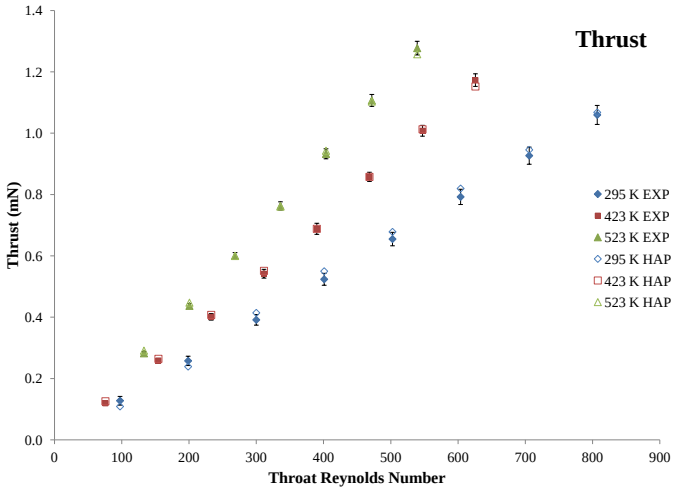

(a) Thrust

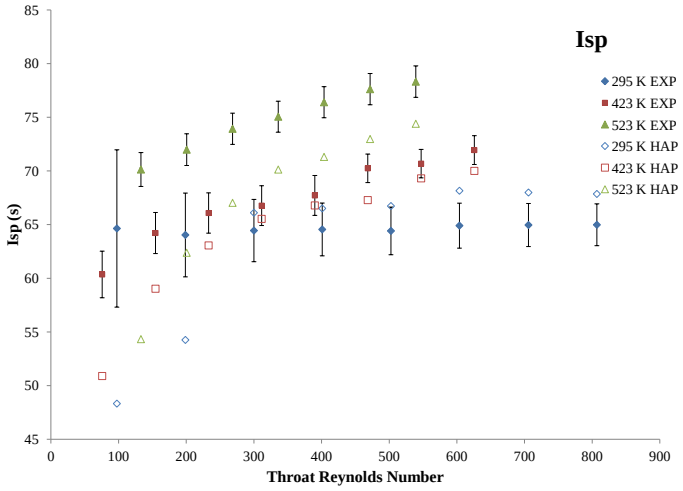

(b) Specific Impulse

Figure 7: Experimental and Numerical Thrust Comparison for the 40-200-0006 Nozzle

margin of error. From Fig. 7(b) it can be observed that HAP under predicts the specific impulse at lower Reynolds number, but compares better for higher Reynolds numbers.

The most likely reason HAP under predicted the experimental thrust in the cold gas test is the number of particles per cell is insufficient. For the most accurate results it is suggested to have 10 or more particles per cell for DSMC simulations. There is a desire to keep the numerical cost as low as possible without sacrificing accuracy.

The data in table 3 gives the experimental and numerical thrust, experimental error and the difference between the numerical and experimental thrust for the three chamber temperatures and eight throat Reynolds numbers. Overall, in 14 out of 23 cases HAP predicted thrust within the margin of experimental error. The largest discrepancy is run 4 in the 295K test which over predicts the experimental result by 26 μN, but is only a little over 6 μN outside the experimental error.

Table 3: Comparison between HAP Results and Experimental Data for 40-200-0006 Nozzle

	Cold Gas Test (295K)				
Run	Re^*	Thrust Exp [mN]	Thrust HAP [mN]	Difference [mN]	Exp Error [mN]
1	97.47	0.1276	0.1088	0.0187	0.0141
2	198.71	0.2576	0.2389	0.0187	0.0153
3	300.02	0.3913	0.4141	0.0228	0.0171
4	400.99	0.5236	0.5498	0.0262	0.0194
5	502.55	0.6547	0.6782	0.0235	0.0220
6	603.79	0.7923	0.8195	0.0272	0.0249
7	705.81	0.9267	0.9457	0.0190	0.0279
8	806.91	1.0596	1.0677	0.0081	0.0310
	Hot Gas Test (423K)				
Run	Re^*	Thrust Exp [mN]	Thrust HAP [mN]	Difference [mN]	Exp Error [mN]
1	75.75	0.1191	0.1258	0.0066	0.0031
2	154.54	0.2586	0.2642	0.0056	0.0068
3	233.04	0.4013	0.4074	0.0061	0.0105
4	311.46	0.5419	0.5511	0.0092	0.0142
5	390.01	0.6883	0.6881	0.0001	0.0181
6	468.28	0.8576	0.8576	0.0000	0.0150
7	547.16	1.0080	1.0127	0.0047	0.0176
8	625.81	1.1731	1.1522	0.0208	0.0205
	Hot Gas Test (523K)				
Run	Re^*	Thrust Exp [mN]	Thrust HAP [mN]	Difference [mN]	Exp Error [mN]
2	133.04	0.2822	0.2910	0.0088	0.0049
3	200.67	0.4370	0.4474	0.0105	0.0076
4	268.46	0.6002	0.5994	0.0007	0.0105
5	335.97	0.7628	0.7604	0.0024	0.0133
6	403.67	0.9327	0.9428	0.0102	0.0163
7	471.75	1.1070	1.1031	0.0039	0.0194
8	539.28	1.2774	1.2574	0.0200	0.0223

IV. Summary

There has been a growth in demand for CubeSats and resulting in a need to increase the efficiency in micro-propulsion resisto-jet systems. Previously, a DSMC method was investigated as a numerical method for optimization of low Reynolds number micro-nozzles. This procedure is advantageous as it accounts for

viscosity and rarefied effects inside the low Reynolds number micro-nozzle. This paper discussed validation of the DSMC code with experimental results for various nozzle geometries across a range of Reynolds numbers using nitrogen propellants at different temperatures.

The U.S. Naval Research Laboratory conducted its own experimental program in parallel with this numerical study. The experimental program started with four nozzle. The nozzles are tested with nitrogen gas at three temperatures; 295K, 423K and 523K. In addition, each nozzle is tested at 8 different flow rates which allowed studying the nozzle over a range of Reynolds number. Unfortunately, only two of the four nozzles, nozzle 60-100-0006 and nozzle 40-200-0006, were able to have all test runs simulated in time to be published in this paper. The remaining two nozzles, nozzle 40-050-0006 and nozzle 40-100-0006, will have all test runs simulated and data will be published at a later date.

In general, the HAP code was able to predict the thrust well. HAP predicted a total of 29 cases out of 47 within the margin of experimental error. The largest discrepancy is run 8 in the 423K test with nozzle 60-100-0006 which HAP over predicts the experimental result by 31 μN, but is only a little over 6 μN outside the experimental error. Another issue that was observed in this study is the high variability in the prediction of specific impulse. It is believed the reason for this variability in specific impulse is due to the fact that specific impulse requires the thrust and mass flux be calculated, and, any error in these calculations, becomes magnified in the calculation for specific impulse.

References

[1]Ahlberg, J. H., Hamilton, S., Migdal, D., and Nilson, E. N., "Truncated Perfect Nozzles in Optimum Design," *ARS Journal*, Vol. 31, No. 5, 1961.

[2]Hoffman, J., "Design of Compressed Truncated Perfect Nozzles," *Journal of Propulsion*, Vol. 3, No. 2.

[3]Rao, G. V. R., "Exhaust Nozzle Contour for Optimum Thrust," *Jornal of Jet Propulsion*, Vol. 28, 1958.

[4]Osborn, M., Holman, T., Rosenberg, D. A., Tuttle, S. G., Williams, L. T., and McDonald, M., "Overcoming Low Nozzle Efficiency: A Test Correlated Numerical Investigation of Low Reynolds Number Micro-Nozzle Flow," *American Institute of Aeronautics and Astronautics*, 2015, 2015 AIAA Propulsion and Energy.

[5]Williams, L. T., McDonald, M., and Osborn, M., "Performance Characterization of a Low Reynolds Number Micro-Nozzle Flow," *American Institute of Aeronautics and Astronautics*, 2015, 2015 AIAA Propulsion and Energy.

[6]Williams, L. T. and Osborn, M., "Performance Impacts of Geometry and Operating Conditions on a Low Reynolds Number Micro-Nozzle Flow," *International Electric Propulsion Conference*, 2017.

[7]Tuesta, A., Fisher, B. T., Williams, L. T., and Osborn, M. F., "Spontaneous Raman Scattering Spectroscopy of a Resistojet Plume in a Vacuum Environment," *International Electric Propulsion Conference*, 2017.

[8]Houssaini, M. M. and Korte, J. J., "Investigation of Low-Reynolds-Number Rocket Nozzle Design Using PNS-Based Optimization Procedure," Technical Memorandum 110295, NASA, 1996.

[9]Minghou, L., Xianfeng, Z., Genxuan, Z., and Yiliang, C., "Study on Micronozzle Flow and Propulsion Performance using DSMC and Continuum Methods," *Acta Mechanica Sinica*, Vol. 22, 2006.

[10]Holman, T. and Osborn, M., "Numerical Optimization of Micro-Nozzle Geometries for Low Reynolds Number Resistojets," *American Institute of Aeronautics and Astronautics*, 2015, 2015 AIAA Propulsion and Energy.

[11]Burt, J. M., Eswar, J., and Boyd, I. D., "A Novel Cartesian Implementation of the Direct Simulation Monte Carol Method," *American Institute of Aeronautics and Astronautics*, 2011, AIAA-2011-632, 49th AIAA ASM Conference, Orlando, FL, Jan. 4-7.

[12]Rosenberg, D. A., Williams, B., Tuttle, S., Osborn, M., and Williams, L. T., "Optical Measurements of Density and Species Concentration in a Low Reynolds Number Micro-Nozzle Flow," *American Institute of Aeronautics and Astronautics*, 2015, 53rd AIAA Aerospace Sciences Meeting.